To the Graduate Council:

I am submitting herewith a thesis written by Andrew William Wilson entitled "Nonlinear Acoustics of Piston-Driven Gas-Column Oscillations." I have examined the final electronic copy of this thesis for form and content and recommend that it be accepted in partial fulfillment of the requirements for the degree of Master of Science, with a major in Aerospace Engineering.

Gary F. Flandro, Major Professor

---

We have read this thesis
and recommend its acceptance:

Trevor M. Moeller

---

Gregory Sedrick

---

Acceptance for the Council

Carolyn R. Hodges

---

Vice Provost and Dean of the Graduate School

(Original signatures are on file with official student records.)

# NONLINEAR ACOUSTICS OF PISTON-DRIVEN GAS-COLUMN OSCILLATIONS

A Thesis

Presented for the

Master of Science

Degree

The University of Tennessee, Knoxville

Andrew William Wilson

August 2010

## Acknowledgments

My thanks go out to Drs. Flandro and Jacob, for letting me build on their work and guiding me through the tangled web of nonlinear acoustic theory; to Drs. Sedrick and Moeller, for their guidance and assistance through the Master's process; to the Church of Christ at Cedar Lane for helping me keep my balance; and to the students of the University of Tennessee Space Institute, for always keeping the debate lively.

Abstract

The piston-driven oscillator is traditionally modeled by directly applying boundary conditions to the acoustic wave equations; with better models re-deriving the wave equations but retaining nonlinear and viscous effects. These better models are required as the acoustic solution exhibits singularity near the natural frequencies of the cavity, with an unbounded (and therefore unphysical) solution. Recently, a technique has been developed to model general pressure oscillations in propulsion systems and combustion devices. Here, it is shown that this technique applies equally well to the piston-driven gas-column oscillator; and that the piston experiment provides strong evidence for the validity of the general theory. Using a modified piston-tube apparatus, agreement between predicted and observed limit-cycle amplitudes is observed to be on the order of 1%.

# Contents

# List of Tables

# List of Figures

# Chapter 1

# Introduction

The experiment seems simple: a sealed tube with a variable-speed piston on one end, and a microphone on the other. Yet at certain frequencies, the observed behavior is quite complex: a steepened, shock-like wave is observed by the microphone when the piston drives at a natural frequency of the tube. The simplest solution to the problem, the acoustic solution, predicts an infinite wave amplitude; and there is no simple solution that accurately predicts the wave amplitude.

Predicting the limit-cycle amplitude of complex, nonlinear pressure oscillations is precisely the aim of recent theories [1] [2] concerning the stability of propulsion systems and combustion devices. That theory, especially when applied to the complex systems it is intended to model, is quite difficult to validate, due to difficulties in obtaining high quality experimental data. But the theory applies to the simpler situation encountered in piston-driven gas column oscillations.

Thus the present hypothesis:

> The nonlinear theory of combustion stability can be used to model piston-driven gas-column oscillations in a closed tube near resonance. Direct experimental data from a sealed tube with a driving piston can be used to validate (or invalidate) this theory.

The initial goal was to use this theory predict the maximum oscillation amplitude observed by Dr. Jacob [3]; follow on work was done to increase the quality of the experiment, as well as to extend the range of parameters covered by experiment, to further validate the theory.

This thesis is organized as follows.

2 The Problem explains how the seemingly solved problem of the driven gas-column relates to deeper, unsolved problems in the field of combustion stability.

3 The Experiment describes the equipment used to obtain new experimental data, in particular obtaining data for different fluids.

4 The Theory summarizes the derivation of the core theory, which can be used to model pressure oscillations in nearly any system.

5 The Theory Applied uses the general theory to derive a relatively simple ordinary differential equation, which models the growth of pressure oscillations in the piston-driven tube experiment.

6 The Results compares the predictions of the theory with the observations from the experiment, and points to where further work would be beneficial.

# Chapter 2

# The Problem

THERE ARE ACTUALLY two problems being addressed; each is the answer to the other. On the one hand there exists the simple experiment, which defies simple analytic modeling, of piston-driven oscillations in a sealed tube. On the other hand, the theory of pressure oscillations in combustion devices is quite complex and defies simple experimental validation. The joint nature of the problem, and the opportunity thus created, is developed as follows:

- 2.1 Present Solutions addresses the issues with present models of the piston-tube experiment, emphasizing what opportunities for improvement are present.
- 2.2 Stability Theory describes the difficulties with combustion stability theories in general, and the nonlinear theory in particular.
- 2.3 The Opportunity shows how these two problems can be used to validate each other.

## 2.1 Present Solutions

In some sense Chester's classical solution [4] provides an excellent example of the problems with current models [5] [6] of piston-driven gas-column oscillations.

First, the classical solution is closely tied to boundary conditions. The model chosen is very symmetric: a cylinder, one end of which is sealed and fixed, and a moving piston on the other end. As will be described in the next chapter, the experiment performed does not meet these boundary conditions–namely, the piston used has a much smaller diameter than the tube itself. Despite the seemingly small nature of this change, it is sufficient to make Chester's theory questionable. To use that approach with the experiment as performed herein, It would be necessary to start near the beginning of his derivation and apply different boundary conditions. Coaxing an analytical solution out of this non-symmetric situation may well be impossible.

This brings out the second difficulty: such explicit analytic solutions do not extend to even simple changes in geometry. Without complete re-derivation, Chester's solution cannot be applied to, for instance, a curved tube with a piston on one end. The procedure is so tied to the geometric assumptions (particularly the symmetry assumptions) that it could not be applied to any system that cannot be reduced to one dimension.

The third issue is that the full solution (including viscous damping) is essentially unusable. As Chester himself says:

> The continuous solutions [of the compressively viscous equation] are adequately represented by [the inviscid solution], and the effect of compressive viscosity on these solutions will not be considered.

Essentially, after 5 pages of dense manipulation of differential equations, and an intensive discussion of why the results of these manipulations are difficult to use and how the manipulations cannot be relied upon due to subtleties in the mathematics, Chester concludes by negating compressive viscosity.

Combined, these issues make the solutions presented for the piston-tube experiment brittle: even small changes in the experiment render them useless, and the math involved makes them incredibly unwieldy for predicting even the original experiment.

## 2.2 Stability Theory

The theories developed for predicting pressure oscillations in combustion devices [7] [8] [1] [9] do not suffer this same brittleness. By necessity, these theories are trying to describe oscillations in all kinds of geometries, under a wide range of fluid-dynamic and thermodynamic conditions. As such, they have broken down the problem into three questions:

1. What oscillations can a particular system support? (An eigenvalue-eigenfunction problem, with the eigenvalues being natural frequencies and the eigenfunctions describing mode shapes).

2. What processes can drive oscillations? What can damp them? (A problem of locating sources and sinks of energy at the natural frequencies).

3. With the known sources and sinks, how will the amplitude of oscillations develop? (A dynamic systems problem, with the answer to be found in linear or nonlinear dynamics).

In breaking down the problem in this manner, the theories have gained a great deal of flexibility. Acoustic theory can be employed, analytically or numerically, to answer the first question. Fluid dynamics, thermodynamics, and even empirical modeling can be employed to address the second. And by using the eigenvalue decomposition, the governing equations can be used to derive *relatively* simple dynamic models.

But with this flexibility comes uncertainty. No dynamic model has ever exactly predicted the behavior of a combustion device in an incontrovertible way. For any given device there is always a way to question the validity of the results. This creates doubts about whether the model has indeed captured the physics of the system. Was vortex-shedding really that important or was it unstable flame-fronts? Was it nozzle-damping or viscous-damping? How good are the measurements of viscosity of these highly-ionized rocket gases? Was the system truly acoustically nonlinear or was that a measurement artifact?

## 2.3 The Opportunity

In this state of affairs, stuck between theories few people will accept and complex experimental data about which no simple theory is credible, an opportunity is created.

In some sense, the piston-driven acoustic tube has many of the characteristics observed in combustion devices: wave-steepening, limit-cycle amplitudes, mean pressure shifts. This analytically well-understood system should be susceptible to the same methods of analysis developed for combustion devices. High-resolution experimental data already exists, [10] [3] and more can be created cheaply.

The present goals are identified: First, to *quantitatively* predict the limit-cycle of the piston-driven acoustic resonator using Dr. Flandro's theory. [1] Second, to build such a resonator and run it under a variety of conditions. And third, to compare the results to past experiments and theories.

# Chapter 3

# The Experiment

Many researches have built piston-driven acoustic resonators. Sanger and Hudson [10] built fairly sophisticated versions to determine resonance mode-shapes and amplitudes. Motivated by the combustion stability problem and recent theoretical work by Jacob [2], the present experiment is intended to obtain high-resolution data for direct theory comparison.

The experimental apparatus was originally developed by Jacob [3] to explore mean pressure shift and wave-steepening. The experiment sought to obtain spectra of driven first-modes from a variety of gases to validate recently developed theoretical results.

## 3.1 Apparatus

Figure 3.1 shows a schematic of the apparatus, and dimensions can be found in Table 3.1.

At one end, a ring of plastic is epoxied to the tube, enabling it to be bolted to a driving source. The driving source is a re-used engine block with the sole piston chamber exposed. This engine block is mounted on the end of the tube so that the piston oscillates in the tube's longitudinal direction (Figure 3.2). The piston itself is driven by an attached variable-speed electric motor.

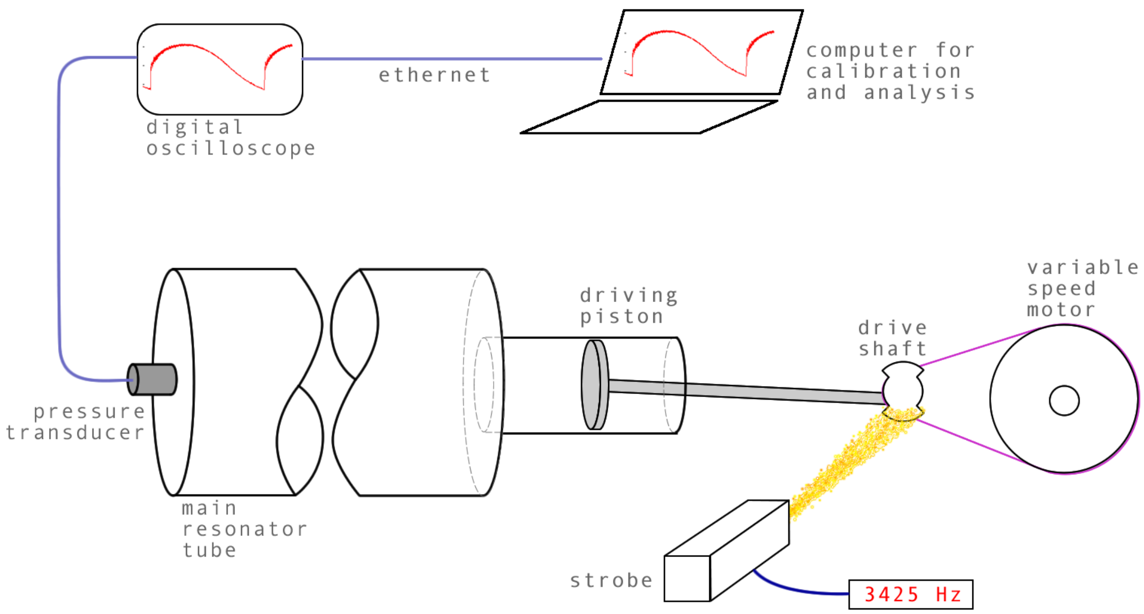


Figure 3.1: Schematic of the experimental apparatus.

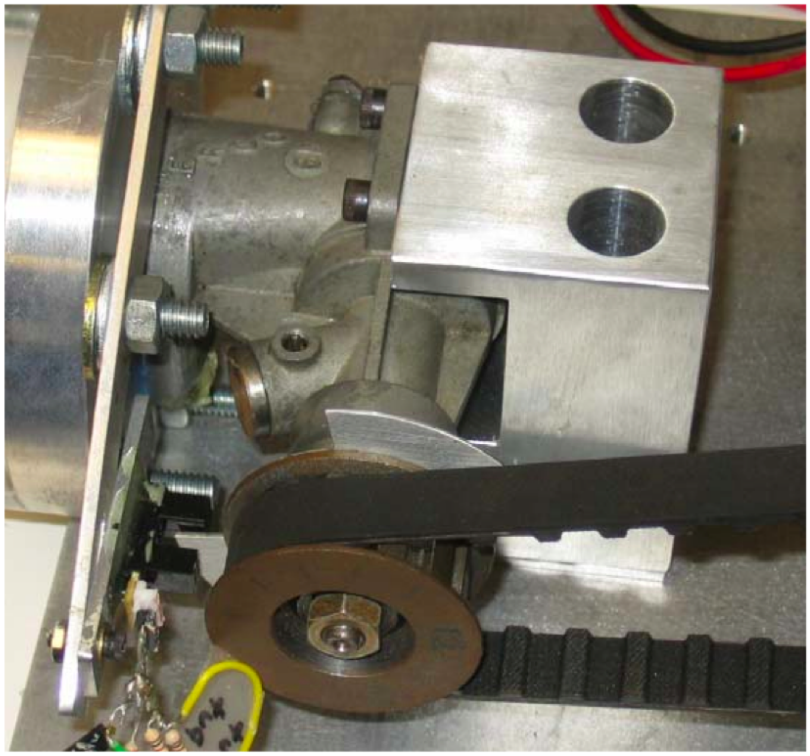

Figure 3.2: Photo of driving piston

Table 3.1: Apparatus dimensions

| | | | | |
|---|---|---|---|---|
| Piston stroke | 7/8 | in | ±1/32 | in |
| Piston diameter | 15/16 | in | ±1/32 | in |
| Tube length | 124 | in | ±1/8 | in |
| Tube inner diameter | 2 | in | ±1/32 | in |
| Max piston frequency | 78.4 | Hz | | |
| Fundamental frequency [air] | 56.2 | Hz | ±0.3 | Hz |

The other end of the tube is sealed with a flat, clear plastic plate, in the center of which is mounted a 2 psi dynamic pressure transducer.

Valves are mounted at either end of the tube, and a 15 psi limited pressure gauge is connected to one of these valves. These valves provide access to pump gasses such as helium and carbon dioxide into the tube, as well as the ability to partially pressurize the tube.

## 3.2 Procedure

The tube was checked for leaks by applying 5 psig of pressure inside the tube and watching the rate of pressure drop. Leaks were found and sealed until the rate was less than 1 psi per minute.

The procedure focused on obtaining data near the first resonant frequency for each of the observed gases (air and $CO_2$). For each gas, the following steps were taken:

1. Flood the tube with the chosen gas, by flowing that gas through the tube until all other gases have been largely displaced.

2. Wait for the tube-gas combination to warm up to room temperature, periodically releasing pressure from the tube to keep it near atmospheric pressure. (The following steps are undertaken immediately, before air has a chance to leak back into the tube).

3. Power on the equipment, and slowly increase the motor speed until the first resonant frequency is heard ($\sim$ 1+ psi waves in the tube result in a very loud buzzing sound).

4. Using the strobe, measure the rotational speed of the cam shaft and hence the frequency of the piston.

5. Using the oscilloscope, observed and capture the voltage oscillations induced in the pressure transducer.

6. Repeat the previous two steps at several points near the resonant frequency.

7. Download the waveform from the oscilloscope to a computer, and apply the pressure transducer calibration (138 mV per psi) to obtain a pressure-time data set.

Clear waveforms were captured for each of the two gases. An example of this data can be seen in Figure 3.3.

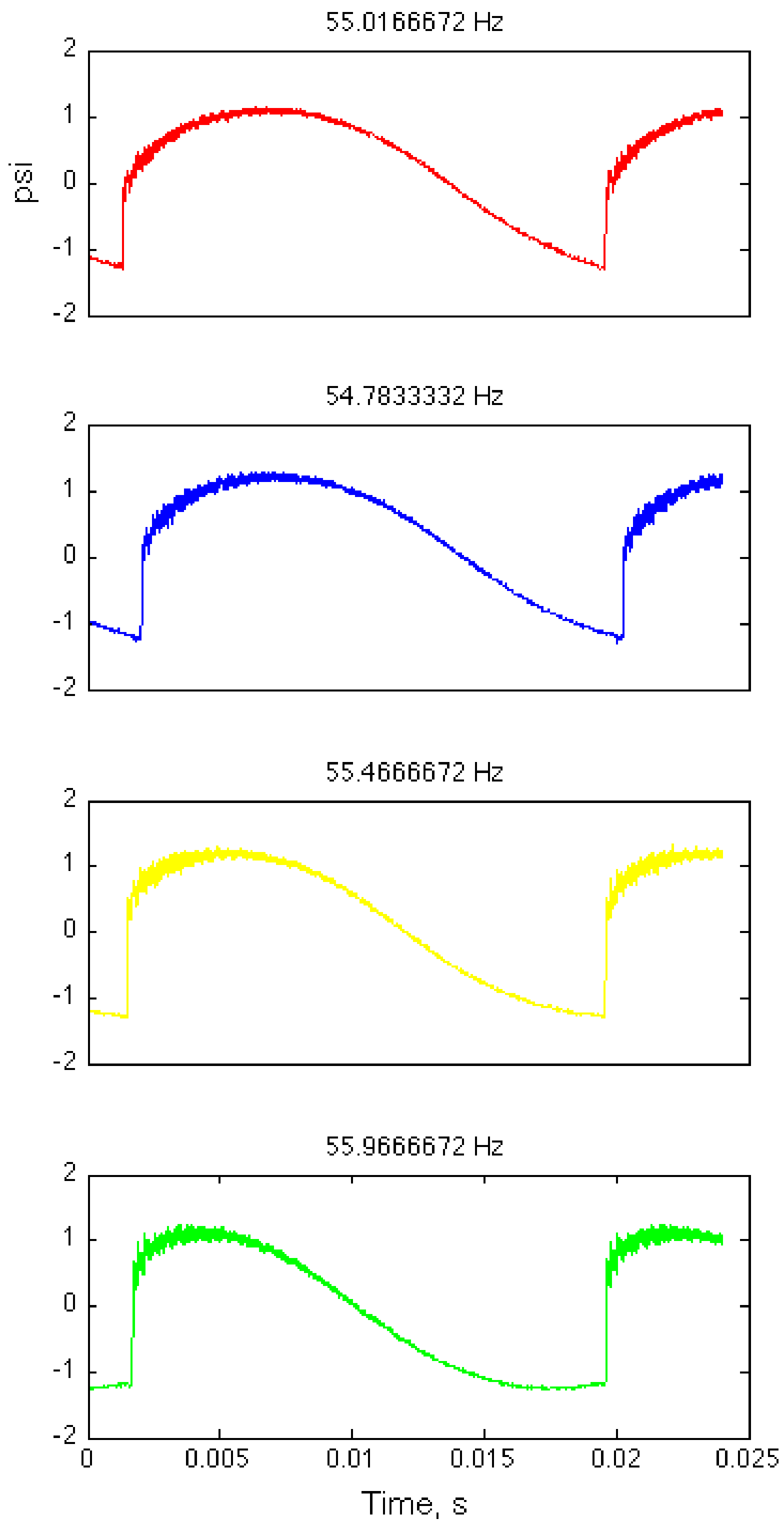


Figure 3.3: Typical shock-like waveforms in air observed near resonance

# Chapter 4

# The Theory

The general theory summarized here is attributed to Flandro [1], based on work by Myers [9] and Cantrall & Hart [8], and exactly follows the version laid out by Jacob [2]. The theory–used to predict the amplitudes and spectra of steepened piston-driven oscillations–is laid out in this chapter as follows.

- In 4.1 Variables and Expansions, a complete set of independent fluid and thermodynamic variables are chosen, and said variables are assumed to have an expanded / perturbed form.
- In 4.2 Defining Equations, an appropriate, closed set of governing equations (fluid dynamic, thermodynamic, and state) are chosen.
- In 4.3 Finalized Energy Balance, the energy balance equation is expanded around the mean (or zeroth-order) variables.
- And in 4.4 1st Order Energy, 4.5 2nd Order Energy, and 4.6 3rd Order Energy, the energy balance equation is examined at each order.

## 4.1 Variables and Expansions

Motivated by a desire to choose the entropy equation (over the energy equation), we choose and expand the independent field variables

$$\vec{u} = \vec{u}_0 + \vec{u}_1 + \vec{u}_2 + \dots \tag{4.1}$$

$$p = p_0 + p_1 + p_2 + \dots \tag{4.2}$$

$$\rho = \rho_0 + \rho_1 + \rho_2 + \dots \tag{4.3}$$

$$T = T_0 + T_1 + T_2 + \dots \tag{4.4}$$

$$s = s_0 + s_1 + s_2 + \dots \tag{4.5}$$

$$\tag{4.6}$$

where

$$\frac{\Xi_i}{\Xi_0} \approx \epsilon^i \tag{4.7}$$

with $\epsilon$ a small quantity ($\ll 1$) and $\Xi \in \{\vec{u}, p, \rho, T, s\}$ .

For convenience, we also define

$$\vec{m} = \vec{m}_0 + \vec{m}_1 + \vec{m}_2 + \dots \tag{4.8}$$

$$\equiv \rho\vec{u} \tag{4.9}$$

$$= (\rho_0 + \rho_1 + \dots)(\vec{u}_0 + \vec{u}_1 + \dots) \tag{4.10}$$

$$= (\rho_0\vec{u}_0) + (\rho_0\vec{u}_1 + \rho_1\vec{u}_0) + \dots \tag{4.11}$$

## 4.2 Defining Equations

Based upon our choice of variables, we require two thermodynamic relations, an equation of state, and five fluid mechanic equations (three for the vector velocity plus density and entropy).

The thermodynamic equations are derived by Liepman and Roshko [11]:

$$dp = \frac{a^2\rho}{c_p}ds + a^2 d\rho \tag{4.12}$$

$$dT = \frac{T}{c_p}ds + \frac{1}{\rho c_p}dp \tag{4.13}$$

We assume a thermally perfect gas with the speed of sound given by

$$a = \sqrt{\gamma RT} \tag{4.14}$$

and further assume an ideal gas so that the equation of state is expressed as

$$p = \rho RT \tag{4.15}$$

The five fluid mechanic equations are continuity, vector momentum (three equations in one vector equation), and entropy:

$$\frac{\partial \rho}{\partial t} + \nabla \cdot \vec{m} = 0 \quad \text{Continuity} \tag{4.16}$$

$$\frac{\partial \vec{u}}{\partial t} + \vec{\omega} \times \vec{u} + \nabla H - T\nabla s = \vec{\psi} \quad \text{Momentum} \tag{4.17}$$

$$\frac{\partial (\rho s)}{\partial t} + \nabla \cdot (\vec{m}s) = Q \quad \text{Entropy} \tag{4.18}$$

The additional variables used in these equations are given in Table 4.1.

Although not required, there are additional thermodynamic relations that are of use in some of the derivations. For completeness, the entire set of thermodynamic relations are summarized in Table 4.2.

Table 4.1: Additional variables and their defining equations.

| | Variable | Defining equation |
|---|---|---|
| $h$ | enthalpy | $h = e + \frac{p}{\rho}$ |
| $e$ | internal energy | $de = T\,ds + \frac{p}{\rho^2}\,d\rho$ |
| $H$ | total enthalpy | $H = h + \frac{1}{2}\vec{u}^2$ |
| $\vec{\omega}$ | vorticity | $\vec{\omega} = \nabla \times \vec{u}$ |
| $\vec{\zeta}$ | lambda vector | $\vec{\zeta} = \vec{\omega} \times \vec{u}$ |
| $Q$ | heat release | $Q = \frac{1}{T}(\Phi - \nabla \cdot \vec{q} + \mathcal{H})$ |
| $\mathcal{H}$ | distributed heat release | |
| $\vec{q}$ | heat transfer | |
| $\vec{\psi}$ | viscous stress | $\vec{\psi} = \frac{1}{\rho}(-\mu\nabla \times \nabla \times \vec{u} + (\eta + \frac{4}{3}\mu)\nabla(\nabla \cdot \vec{u}) + \vec{F})$ |
| $\vec{F}$ | body force | |
| $\Phi$ | viscous dissipation | $P_{ij}\frac{\partial u_j}{\partial x_i}$ |
| $P_{ij}$ | transposed stress tensor | $P_{ij} = \sigma'_{ij} = \mu\left(\frac{\partial v_i}{\partial x_j} + \frac{\partial v_j}{\partial x_i} - \frac{2}{3}\delta_{ik}\frac{\partial v_l}{\partial x_l}\right) + \eta\delta_{ik}\frac{\partial v_l}{\partial x_l}$ |

Table 4.2: The thermodynamic relations.

| Symbol | Variable | Relation |
|---|---|---|
| $e$ | internal energy | $de = T\,ds + \frac{p}{\rho^2}\,d\rho$ |
| $h$ | enthalpy | $T\,ds + \frac{1}{\rho}\,dp$ |
| | | $\gamma T\,ds + \frac{a^2}{\rho}\,d\rho$ |
| $p$ | pressure | $dp = \frac{a^2\rho}{c_p}\,ds + a^2\,d\rho$ |
| $T$ | temperature | $dT = \frac{T}{c_p}\,ds + \frac{1}{\rho c_p}\,dp$ |
| | | $dT = \frac{1}{c_p}(\gamma T\,ds + \frac{a^2}{\rho}\,d\rho)$ |

## 4.3 Finalized Energy Balance

By applying the zeroth order equations, Dr. Jacob finds the energy balance to be

$$\frac{\partial E}{\partial t} + \nabla \cdot \vec{W} = D \tag{4.19}$$

with

$$E = \rho\left((H - H_0 - T_0(s - s_0)\right) - \vec{m}_0 \cdot (\vec{u} - \vec{u}_0) - (p - p_0) \tag{4.20}$$

$$\begin{aligned} W = {} & (\vec{m} - \vec{m_0})\left((H - H_0) + T_0(s - s_0)\right) + \vec{m}_0(T - T_0)(s - s_0) \\ & - (m_j - m_{0j})\left(\frac{P_{ij}}{\rho} - \frac{P_{0ij}}{\rho_0}\right) + (T - T_0)\left(\frac{\vec{q}}{T} - \frac{\vec{q}_0}{T_0}\right) \end{aligned} \tag{4.21}$$

$$\begin{aligned} D = {} & \vec{m} \cdot \vec{\zeta}_0 + \vec{m}_0 \cdot \vec{\zeta} - (s - s_0)\vec{m} \cdot \nabla T_0 + (s - s_0)\vec{m}_0 \cdot \nabla T \\ & - \left(\frac{P_{ij}}{\rho} - \frac{P_{0ij}}{\rho_0}\right)\frac{\partial}{\partial x_i}(m_j - m_{0j}) \\ & + (m_j - m_{0j})\left(\frac{P_{ij}}{\rho^2}\frac{\partial \rho}{\partial x_i} - \frac{P_{0ij}}{\rho_0^2}\frac{\partial \rho_0}{\partial x_i}\right) \\ & + (T - T_0)\left(\frac{\phi}{T} - \frac{\phi_0}{T_0}\right) + \left(\frac{\vec{q}}{T} - \frac{\vec{q}_0}{T_0}\right) \cdot \nabla(T - T_0) \\ & - (T - T_0)\left(\frac{\vec{q} \cdot \nabla T}{T^2} - \frac{\vec{q}_0 \cdot \nabla T_0}{T_0^2}\right) \end{aligned} \tag{4.22}$$

## 4.4 1st Order Energy

When the completely expanded variables are substituted into the energy balance, Dr. Jacob shows that the energy balance equation to first order

$$\frac{\partial E_1}{\partial t} + \nabla \cdot \vec{W}_1 = D_1 \tag{4.23}$$

collapses to $0 = 0$; that is, the expansion itself satisfies the first order energy constraint and reveals no relationships between the first order variables.

## 4.5 2nd Order Energy

The second order equation establishes relationships between the first order variables:

$$\frac{dE_2}{dt} + \nabla \cdot \overrightarrow{W_2} = D_2 \tag{4.24}$$

where

$$E_2 = \frac{p_1^2}{2\rho_0 a_0^2} + \rho_1(\vec{u}_0 \cdot \vec{u}_1) + \frac{1}{2}\rho_0(\vec{u}_1 \cdot \vec{u}_1) + \frac{\rho_0 T_0}{2c_P} s_1^2 \tag{4.25}$$

$$\vec{W}_2 = \vec{m}_1(h_1 + \vec{u}_0 \cdot \vec{u}_1) - \vec{m}_1 T_0 s_1 + \vec{m}_0 T_1 s_1 \tag{4.26}$$

$$\begin{aligned} D_2 = {} & \vec{m}_1 \cdot \vec{\psi}_1 + T_1 Q_1 - \vec{m}_1 s_1 \cdot \nabla T_0 + \vec{m}_0 s_1 \cdot \nabla T_1 \\ & - \rho_0 \vec{u}_0 \cdot (\vec{u}_1 \times \vec{\omega}_1) - \rho_1 \vec{u}_1 \cdot (\vec{u}_0 \times \vec{\omega}_0) \end{aligned} \tag{4.27}$$

## 4.6 3rd Order Energy

The full (and extensive) third-order energy balance result derived by Dr. Jacob, establishes some relationships among second-order variables. But the third-order energy term itself reveals an additional relationship between first-order variables:

$$E_3 = \frac{1}{2}\rho_1 \vec{u}_1^2 + \frac{1 - 2\gamma)p_1^3}{6p_0^2 a_0^4} \tag{4.28}$$

This highly nonlinear coupling results in coupling between the various acoustic modes.

# Chapter 5

# The Theory Applied

FOLLOWING THE STANDARD combustion-theory modeling approach, there are three questions:

1. What modes will support oscillations?
2. What drives or damps at the corresponding frequencies?
3. How will the oscillation amplitude(s) evolve in time?

5.1 Assumptions documents the assumptions made about the system.

5.2 Acoustic Decomposition answers the first question, finding the net pressure fluctuation decomposed into individual modes,

$$p_1 = \sum_{n=1}^{\infty} \underbrace{R_n}_{\text{amplitude}} * \underbrace{\sin(\omega_n t)}_{\text{temporal mode shape}} * \underbrace{\psi_n(\vec{r})}_{\text{spatial mode shape}} \tag{5.1}$$

In 5.3 Energy Balance, 5.4 Source: Piston-Driving Work, 5.5 Sink: Viscous Boundary Layer Losses, and 5.6 Sink: Compressive Viscous Losses, this expansion is then substituted into the expanded terms of the energy balance equation. Evaluating each term determines where energy is being added to or removed from the fluctuations; thus answering the second question.

Finally, in 5.7 Dynamic Model, the resulting terms are time averaged and volume-integrated, isolating the the amplitude functions $\{R_n\}$. This gives a dynamic model for amplitude evolution in time, which classically looks like

$$\dot{R}_n = \underbrace{\left(\sum_j \alpha_{n,j}\right) R_n}_{\text{feedback sources and sinks}} \underbrace{- \frac{2-\gamma}{8\gamma}\omega_n \sum_{l,m=1}^{\infty} E_{n,l,m} R_l R_m}_{\text{nonlinear mode coupling}} \tag{5.2}$$

As will be shown, this dynamic model is missing a class of terms relating to direct driving, but naturally extends to include them.

Note that for the sake of compactness, volume integration and time-averaging is applied to each term as it is manipulated.

## 5.1 Assumptions

For the acoustic tube with no mean flow, we assume:

$$\vec{u}_0 \equiv 0 \qquad \text{no mean flow} \tag{5.3}$$

$$s_1 \equiv 0 \qquad \text{entropy fluctuations negligible} \tag{5.4}$$

$$\vec{\omega}_0 \equiv 0 \qquad \text{irrotational mean flow (from no mean flow)} \tag{5.5}$$

Further, assume that the piston is driving at the first resonant frequency $\omega_1$.

## 5.2 Acoustic Decomposition

Following Jacob [2] and based on the work of Quarteroni et al. [12], the decomposition for a long, thin tube is a standard Galerkin spectral decomposition:

$$p_1 = p_0 \sum_{n=1}^{\infty} \eta_n(t)\psi_n(\vec{r}) \tag{5.6}$$

$$u_1 = \sum_{n=1}^{\infty} \frac{1}{\gamma k_n^2} \dot{\eta}_n(t) \nabla \psi_n(\vec{r}) \tag{5.7}$$

$$\eta_n = R_n \sin(\omega_n t) \tag{5.8}$$

$$\psi_n = \cos(k_n x) \tag{5.9}$$

$$\omega_n = 2\pi \frac{a_0}{L} \tag{5.10}$$

$$k_n = \frac{\omega_n}{a_0} \tag{5.11}$$

## 5.3 Energy Balance

The $2^{nd}$ order energy balance is the method for determining the sources and sinks of acoustic energy:

$$\frac{dE_2}{dt} + \nabla \cdot \overrightarrow{W_2} = D_2 \tag{5.12}$$

where

$$E_2 = \frac{p_1^2}{2\rho_0 a_0^2} + \rho_1(\vec{u}_0 \cdot \vec{u}_1) + \frac{1}{2}\rho_0(\vec{u}_1 \cdot \vec{u}_1) + \frac{\rho_0 T_0}{2c_P} s_1^2 \tag{5.13}$$

$$\vec{W}_2 = \vec{m}_1(h_1 + \vec{u}_0 \cdot \vec{u}_1) - \vec{m}_1 T_0 s_1 + \vec{m}_0 T_1 s_1 \tag{5.14}$$

$$\begin{aligned} D_2 = {} & \vec{m}_1 \cdot \vec{\psi}_1 + T_1 Q_1 - \vec{m}_1 s_1 \cdot \nabla T_0 + \vec{m}_0 s_1 \cdot \nabla T_1 \\ & - \rho_0 \vec{u}_0 \cdot (\vec{u}_1 \times \vec{\omega}_1) - \rho_1 \vec{u}_1 \cdot (\vec{u}_0 \times \vec{\omega}_0) \end{aligned} \tag{5.15}$$

Jacob derived the quasi-steady rate-of-change of the total energy to be

$$\frac{\partial}{\partial t} \left\langle \int_V E_2 dV \right\rangle = \frac{ALp_0}{4\gamma} \sum_{n=1}^{\infty} \frac{\partial}{\partial t}(R_n^2) \tag{5.16}$$

which, when used with equation 5.12, hints at the left-hand side of the anticipated differential equation ($R' = \alpha R$):

$$\sum_{n=1}^{\infty} R_n R_n' = \frac{2\gamma}{ALp_0}\left(D_2 - \nabla \cdot \vec{W}_2\right) \tag{5.17}$$

What remains is to evaluate the sources and sinks contained in the work term $\nabla \cdot \vec{W}_2$ and the source term $D_2$, accounting for the influence of processes like viscosity, heat transfer, and piston-driving.

## 5.4 Source: Piston-Driving Work

The previous work with this theory has focused in the self-excited oscillations common in combustion devices. Here, the primary source of oscillating energy is the work done by the piston. The theory has never been used before with systems that have direct piston-driving; so the work term needs to be evaluated and the procedure applied.

The work term $\overrightarrow{W}_2$ in the second order energy balance is given by

$$\overrightarrow{W}_2 = \vec{m}_1(h_1 + \vec{u}_0 \cdot \vec{u}_1) - \vec{m}_1 T_0 s_1 + \vec{m}_0 T_1 s_1 \tag{5.18}$$

Table 5.1 inserts expansions and assumptions into this expression for $\vec{W}_2$, which simplifies to

$$\vec{W}_2 = \vec{u}_1 p_1 \tag{5.19}$$

Integrating to get the total rate of work done, and applying the divergence theorem,

$$\int_V \nabla \cdot \vec{W}_2 \, dV = \int_S \hat{n} \cdot (\vec{u}_1 p_1) \, dS \tag{5.20}$$

Now, $\vec{u}_1$ vanishes everywhere except on the surface of the piston, which has area $A_p$, stroke length $2l$, position $x_p = l\cos(\omega_1 t)$, and velocity $u_p = -l\omega \sin(\omega_1 t)$. Substituting this

Table 5.1: Assumptions and expansions applied to $\vec{W}_2$.

| $\overrightarrow{W}_2$ | substitution | reason |
|---|---|---|
| $\vec{m}_1(h_1+\vec{u}_0\cdot\vec{u}_1)-\vec{m}_1T_0s_1+\vec{m}_0T_1s_1$ | | Second order energy |
| $\vec{m}_1(h_1+\vec{u}_0\cdot\vec{u}_1)-\vec{m}_1T_0s_1+\vec{m}_0T_1s_1$ | $s_1\equiv 0$ | Entropy fluctuations neglected |
| $\vec{m}_1(h_1+\vec{u}_0\cdot\vec{u}_1)$ | | |
| $\vec{m}_1(h_1+\vec{u}_0\cdot\vec{u}_1)$ | $\vec{u}_0\equiv 0$ | No mean flow |
| $\vec{m}_1h_1$ | | |
| $(\rho_0\vec{u}_1+\rho_1\vec{u}_0)h_1$ | $\vec{m}_1=\rho_0\vec{u}_1+\rho_1\vec{u}_0$ | From variable expansion |
| $(\rho_0\vec{u}_1+\rho_1\vec{u}_0)h_1$ | | |
| $(\rho_0\vec{u}_1+\rho_1\vec{u}_0)h_1$ | $\vec{u}_0\equiv 0$ | No mean flow |
| $\rho_0\vec{u}_1h_1$ | | |
| $\rho_0\vec{u}_1\left(\frac{p_1}{\rho_0}+\left(\gamma T_1-\frac{a_0^2}{c_P}\right)s_1\right)$ | $h_1=\frac{p_1}{\rho_0}+\left(\gamma T_1-\frac{a_0^2}{c_P}\right)s_1$ | From variable expansion |
| $\rho_0\vec{u}_1\left(\frac{p_1}{\rho_0}+\left(\gamma T_1-\frac{a_0^2}{c_P}\right)s_1\right)$ | | |
| $\rho_0\vec{u}_1\left(\frac{p_1}{\rho_0}+\left(\gamma T_1-\frac{a_0^2}{c_P}\right)s_1\right)$ | $s_1\equiv 0$ | Entropy fluctuations neglected |
| $\rho_0\vec{u}_1\frac{p_1}{\rho_0}$ | | |
| $\rho_0\vec{u}_1\frac{p_1}{\rho_0}$ | | (canceling) |
| $\vec{u}_1p_1$ | | |

and the spectral expansion for $p_1$,

$$
\begin{aligned}
-\int_S \vec{W}_2\cdot\hat{n}dS &= -A_pu_pp_1 \\
&= A_pl\omega_1\sin(\omega_1 t)p_1 \\
&= A_p\omega_1\sin(\omega_1 t)p_0\sum_{n=1}^{\infty}\eta_n(t)\psi_n(x=0) \\
&= A_pl\omega_1p_0\sum_{n=1}^{\infty}\sin(\omega_1 t)\sin(\omega_n t)R_n(t) \qquad (5.21)
\end{aligned}
$$

Applying time averaging over the period $\tau = \frac{1}{\omega_1}$,

$$\begin{aligned}\left\langle -\int_S \vec{W}_2 \cdot \hat{n} dS \right\rangle &= A_p l \omega_1 p_0 \sum_{n=1}^{\infty} \langle \sin(\omega_1 t) \sin(\omega_n t) R_n(t) \rangle \\ &= A_p l \omega_1 p_0 \sum_{n=1}^{\infty} \frac{1}{\tau} \int_0^{\tau} \sin(\omega_1 t) \sin(\omega_n t) R_n(t) dt \end{aligned} \tag{5.22}$$

$R_n$ is assumed to be a slow function of $t$; that is, we assume the amplitude $R_n$ does not change significantly over a single oscillation period $\tau$. Also,

$$\frac{1}{\tau} \int_0^{\tau} \sin(\omega_1 t) \sin(\omega_n t) = \delta_{1,n} \frac{1}{2} \tag{5.23}$$

since $\omega_n = n \cdot \omega_1$. Finally,

$$\left\langle -\int_S \vec{W}_2 \cdot \hat{n} dS \right\rangle = A_p l \omega_1 p_0 \sum_{n=1}^{\infty} R_n \delta_{1,n} \frac{1}{2} \tag{5.24}$$

To compute the associated alpha, set this equal to the time dependent total energy change (equation 5.16),

$$\frac{ALp_0}{4\gamma} \sum_{n=1}^{\infty} \frac{\partial}{\partial t}(R_n^2) = A_p l \omega_1 p_0 \sum_{n=1}^{\infty} R_n \delta_{1,n} \frac{1}{2} \tag{5.25}$$

Comparing term-by-term, expanding the derivative and moving all constants to the right-hand side, $\dot{R}_n = 0$ for $n \geq 2$, and

$$\dot{R}_1 = \frac{A_p}{A} \frac{l}{L} \gamma \omega_1 \tag{5.26}$$

This new result is *not* the usual form of the $\alpha$ constant. However, this result makes sense. The equation $R' = \alpha R$ is a feedback equation, where the change in oscillations depends upon the already existing oscillations. But this is a driven system, and therefore energy will be added whether oscillations currently exist or not. Hence a constant term–independent of the state of the system–modifying the equation: $\dot{R}_n = \alpha_n R_n + \zeta_n$. With the problem stated like this, the constant associated with driving is given by

$$\zeta_n = \begin{cases} \frac{A_p}{A}\frac{l}{L}\gamma\omega_1, & n = 1 \\ 0, & n > 1 \end{cases} \tag{5.27}$$

This equation predicts a linear, unbounded rise in amplitude at the driven resonant frequency, only with no other frequencies excited. It requires the dynamic nonlinear model and (as yet unaccounted-for) viscous damping to prevent this non-physical result.

## 5.5 Sink: Viscous Boundary Layer Losses

In his textbook, Culick [7] derives the growth constant $\alpha$ due to viscous losses in the acoustic boundary layer of a cylinder. For the sake of brevity the derivation will not be repeated here. Rather, it can be shown that the boundary layer growth constant is given by:

$$\alpha_{bl,n} = -\frac{1}{R_t}\sqrt{\frac{\omega_n \nu}{2}}\left(1 + \frac{\gamma - 1}{\sqrt{Pr}}\right) \tag{5.28}$$

## 5.6 Sink: Compressive Viscous Losses

Morse and Ingard [13] derive the rate of energy loss per unit volume $D_{cv}$ due to the effects of compressive viscosity in an acoustic wave to be

$$D_{cv} = (\eta + \frac{4}{3}\mu)\left\langle\left|\frac{du_x}{dx}\right|^2\right\rangle \tag{5.29}$$

Applying the same process to this source term, we substitute our spectral expansion, time average, and volume integrate.

The oscillating velocity $\vec{u}_1$ expands as

$$\begin{aligned}
\vec{u}_1 &= \sum_{n=1}^{\infty} \frac{1}{\gamma k_n^2} \dot{\eta}_n(t) \nabla \psi_n(\vec{r}) \\
&= \sum_{n=1}^{\infty} \frac{1}{\gamma k_n^2} \frac{d}{dt} \left(R_n \sin(\omega_n t)\right) \nabla \psi_n(\vec{r}) \\
&= \sum_{n=1}^{\infty} \frac{1}{\gamma k_n^2} R_n \omega_n \cos(\omega_n) \nabla \psi_n(\vec{r}) \\
&= \sum_{n=1}^{\infty} \frac{1}{\gamma k_n^2} R_n \omega_n \cos(\omega_n t) \nabla \cos(k_n x) \\
&= \sum_{n=1}^{\infty} \frac{1}{\gamma k_n^2} R_n \omega_n \cos(\omega_n t) (-k_n \sin(k_n x)) \\
&= \sum_{n=1}^{\infty} \frac{1}{\gamma k_n^2} R_n k_n a_0 \cos(\omega_n t) (-k_n \sin(k_n x)) \\
&= \sum_{n=1}^{\infty} \frac{-a_0 k_n^2}{\gamma k_n^2} R_n \cos(\omega_n t) \sin(k_n x) \\
&= \sum_{n=1}^{\infty} \frac{-a_0}{\gamma} R_n \cos(\omega_n t) \sin(k_n x)
\end{aligned} \tag{5.30}$$

Substituting this into $D_{cv}$ (and defining a convenience constant $\Xi \equiv \eta + \frac{4}{3}\mu$):

$$\begin{aligned}
D_{cv} &= \Xi \left\langle \left| \frac{du_x}{dx} \right|^2 \right\rangle \\
&= \Xi \left\langle \left| \sum_{n=1}^{\infty} \frac{-a_0}{\gamma} R_n \cos(\omega_n t) k_n \cos(k_n x) \right|^2 \right\rangle \\
&= \Xi \frac{a_0^2}{\gamma^2} \sum_{n=1}^{\infty} \sum_{m=1}^{\infty} R_n R_m k_n \cos(k_n x) k_m \cos(k_m x) \left\langle \cos(\omega_n t) \cos(\omega_m t) \right\rangle \\
&= \Xi \frac{a_0^2}{\gamma^2} \sum_{n=1}^{\infty} \sum_{m=1}^{\infty} R_n R_m k_n k_m \cos(k_n x) \cos(k_m x) \delta_{m,n} \frac{1}{2} \\
&= \Xi \frac{a_0^2}{2\gamma^2} \sum_{n=1}^{\infty} R_n^2 k_n^2 \cos^2(k_n x) \\
&= \Xi \frac{a_0^2}{2\gamma^2} \sum_{n=1}^{\infty} R_n^2 \frac{\omega_n^2}{a_0^2} \cos^2(k_n x) \\
&= \Xi \frac{1}{2\gamma^2} \sum_{n=1}^{\infty} R_n^2 \omega_n^2 \cos^2(k_n x)
\end{aligned} \tag{5.31}$$

Finally, volume integrating this to get the total power loss to compressive viscosity,

$$\begin{aligned}
\left\langle \int_V D_{cv} dV \right\rangle &= \int_V \Xi \left\langle \left| \frac{du_x}{dx} \right|^2 \right\rangle dV \\
&= \int_V \left( \Xi \frac{1}{2\gamma^2} \sum_{n=1}^{\infty} R_n^2 \omega_n^2 \cos^2(k_n x) \right) dV \\
&= \Xi \frac{1}{2\gamma^2} \sum_{n=1}^{\infty} R_n^2 \omega_n^2 \int_V \cos^2(k_n x) dV \\
&= \Xi \frac{1}{2\gamma^2} \sum_{n=1}^{\infty} R_n^2 \omega_n^2 \int_0^L \cos^2(k_n x) A\, dx \\
&= \Xi \frac{1}{2\gamma^2} \sum_{n=1}^{\infty} R_n^2 \omega_n^2 \frac{A\, L}{2} \\
&= (\eta + \frac{4}{3}\mu) \frac{A\, L}{4\gamma^2} \sum_{n=1}^{\infty} \omega_n^2 R_n^2 \qquad (5.32)
\end{aligned}$$

Comparing this with the energy term (equation 5.16),

$$\frac{ALp_0}{4\gamma} \sum_{n=1}^{\infty} \frac{\partial}{\partial t}(R_n^2) = (\eta + \frac{4}{3}\mu) \frac{L}{4\gamma^2} \sum_{n=1}^{\infty} \omega_n^2 R_n^2 \qquad (5.33)$$

and then comparing term-by-term:

$$\begin{aligned}
\frac{ALp_0}{2\gamma} \dot{R}_n R_n &= (\eta + \frac{4}{3}\mu) \frac{A\, L}{4\gamma^2} \omega_n^2 R_n^2 \\
\dot{R}_n &= \frac{\eta + \frac{4}{3}\mu}{2p_0\gamma} \omega_n^2 R_n \qquad (5.34)
\end{aligned}$$

This gives the compressive viscosity damping alpha for each mode $n$,

$$\alpha_{cv,n} = \left( \eta + \frac{4}{3}\mu \right) \frac{\omega_n^2}{2p_0\gamma} \qquad (5.35)$$

Using the ideal gas law relation for mean variables $p_0 = \rho_0 R T_0$, the nondimensional second coefficient of viscosity $\gamma_{II} = \frac{\eta}{\mu}$, the speed of sound relation $a_0^2 = \gamma R T$, and the kinematic

$\nu = \mu/\rho_0$, we have

$$\begin{aligned}\alpha_{cv} &= (\gamma_{II} + 4/3)\mu \frac{\omega_n^2}{2\rho_0 R T_0 \gamma} \\ &= (\gamma_{II} + 4/3)\frac{\mu}{\rho_0}\frac{\omega_n^2}{2a_0^2} \\ &= (\gamma_{II} + 4/3)\nu \frac{\omega_n^2}{2a_0^2} \end{aligned} \tag{5.36}$$

This newly derived result is applicable to total energy losses in gas-column oscillations. However, it compares exactly with the viscous portion of the "classical acoustic absorbtion coefficient", quoted here from Ingard [13]:

$$a = (\gamma_{II} + \frac{4}{3})\nu \frac{\omega^2}{a_0^3} \tag{5.37}$$

The absorption coefficient is power lost per unit of distance traveled. Multiplying by the wave speed $a_0$, it becomes the power lost per unit of time elapsed, and is exactly the same as the $\alpha$ derived above.

## 5.7 Dynamic Model

Following Flandro (and applying the changes required by driving), the dynamic model becomes:

$$\dot{R}_n = \underbrace{\left(\sum_j \alpha_{n,j}\right) R_n}_{\text{feedback sources and sinks}} + \underbrace{\sum_k \zeta_{n,k}}_{\text{forced sources and sinks}} \underbrace{- \frac{2-\gamma}{8\gamma}\omega_n \sum_{l,m=1}^{\infty} E_{n,l,m} R_l R_m}_{\text{nonlinear mode coupling}} \tag{5.38}$$

Substituting our $\alpha$'s (equations 5.28 and 5.36) and our $\zeta$ (equation 5.27) into this dynamic model, we obtain the specific dynamic model for the piston-driven system:

$$\begin{aligned}\dot{R}_n = &\left(-\frac{1}{R_t}\sqrt{\frac{\omega_n \nu}{2}}\left(1 + \frac{\gamma - 1}{\sqrt{Pr}}\right) + \left(\eta + \frac{4}{3}\mu\right)\frac{\omega_n^2}{2p_0\gamma}\right) R_n \\ &+ \zeta_n - \frac{2-\gamma}{8\gamma}\omega_n \sum_{l,m=1}^{\infty} E_{n,l,m} R_l R_m \end{aligned} \tag{5.39}$$

with

$$\zeta_n = \begin{cases} \frac{A_p}{A}\frac{l}{L}\gamma\omega_1, & n = 1 \\ 0, & n > 1 \end{cases} \tag{5.40}$$

$$\omega_n = \frac{2n\pi a_0}{L} \tag{5.41}$$

$$E_{n,l,m} = \delta(m-n-l) + \delta(m+n-l) - \delta(m-n+l) \tag{5.42}$$

Using appropriate values of the geometry and working fluid constants, this equation is solved numerically for $\{R_n\}$ using a fourth-order Runge-Kutta routine.

# Chapter 6

# The Results

## 6.1 Previous Experiment

The initial goal was to predict the maximum oscillation amplitude observed by Dr. Jacob [3]. Figure 6.1 shows the results of the Dr. Jacob's experiment and the numerical solution to equation 5.39 for that setup; the comparison is quite promising.

## 6.2 Present Experiment

Figures 6.2 and 6.3 show the predicted and measured pressure oscillations for air and carbon dioxide, respectively. In both figures, the measured waveforms and the predicted waveforms are translated so that their minima coincide, by subtracting from each the difference between their respective minima and the minimum of the prediction. Phase is unmeasured, so the waveforms are shown with coinciding phases.

The theory slightly under-predicts the maximum pressure oscillation. However, the difference is on the order of 1%. By comparison, Chester quotes his prediction of Saenger's amplitude as 23.5 cm Hg, and Saenger observed 21.6 cm Hg, a 9% over-prediction.

## 6.3 Conclusions

The general theory for nonlinear pressure oscillations was successfully adapted to the task of predicting the behavior of piston-driven gas-column oscillations in a sealed tube.

Quantitatively, the theory predicted the maximum oscillation amplitude remarkably well. In both cases, the predicted maximum peak-to-trough amplitude was within 1% of the observed value. For air, the closest waveform was 0.73% higher, and .08% higher for carbon dioxide. Due to difficulties in the experimental setup (the inability to produce stable driving frequencies), it was not possible to do a rigorous statistical analysis on waveforms or spectra to determine how closely the theory predicted the exact behavior of the oscillator.

There are some clear possibilities for further work in all domains; but two things seem clear: (1) the nonlinear theory of combustion stability is substantially reliable in predicting peak-to-peak pressure amplitudes; and (2) the piston-tube experiment is a fertile ground for validation of such theories.

## 6.4 Future Work

There are four primary places for future work on this topic: experimental, analytic, numeric, and comparative.

Experimentally, the sources of measurement error need to be reduced. This is especially true for the driving motor, which did not provide stable speeds for any length of time. The goal here would be to produce very stable waveforms in the system, and to measure those waveforms very precisely, in order to be able to produce high quality spectral analysis. Although it can be said that the theory predicts the peak amplitudes of oscillations (for this system) reliably, true validation lies in spectral analysis: The question remains if the theory accurately predict the limit-cycle amplitudes of every excited mode.

Additionally, experiments should be done under different conditions, to cover the range of the relevant parameters: $\gamma$, $Pr$ and $\mu$ can be varied with different gases, and $T$ should be varied to get data at different speeds of sound.

Analytically, the analysis must be extended to cover non-resonant cases. This will involve re-examining the spectral decomposition, as non-resonant eigenvalues create conditions under which non-resonant modes are supported.

Additionally, there is a need is to tighten up the possible sources of error in the predictions. Chief among these are difficulties in locating second coefficient of viscosity $\gamma_{II}$ data for real gases, and accounting for the fact that a cam-piston arrangement does not provide pure sinusoidal driving.

Numeric results exhibit strange behavior due to their inability to model an infinite number of modes. Strictly speaking, there should be no need of viscous damping for the system to reach a limit cycle amplitude; but when run without damping, some of the mode amplitudes go negative. Although the system can be forced to remain positive, there should be no need to do so, and sufficient damping terms always correct the problem. Work needs to be done to determine the source of this numeric irregularity, and to correct it at the analytical level.

Comparatively, the predictions of this model should be compared with the predictions of the classical solutions (e.g., Chester's). This, however, is non-trivial, as those solutions were derived in forms that were essentially unusable, and require a great deal of careful analytical work to get from the stated solution to a usable form of the pressure oscillation.

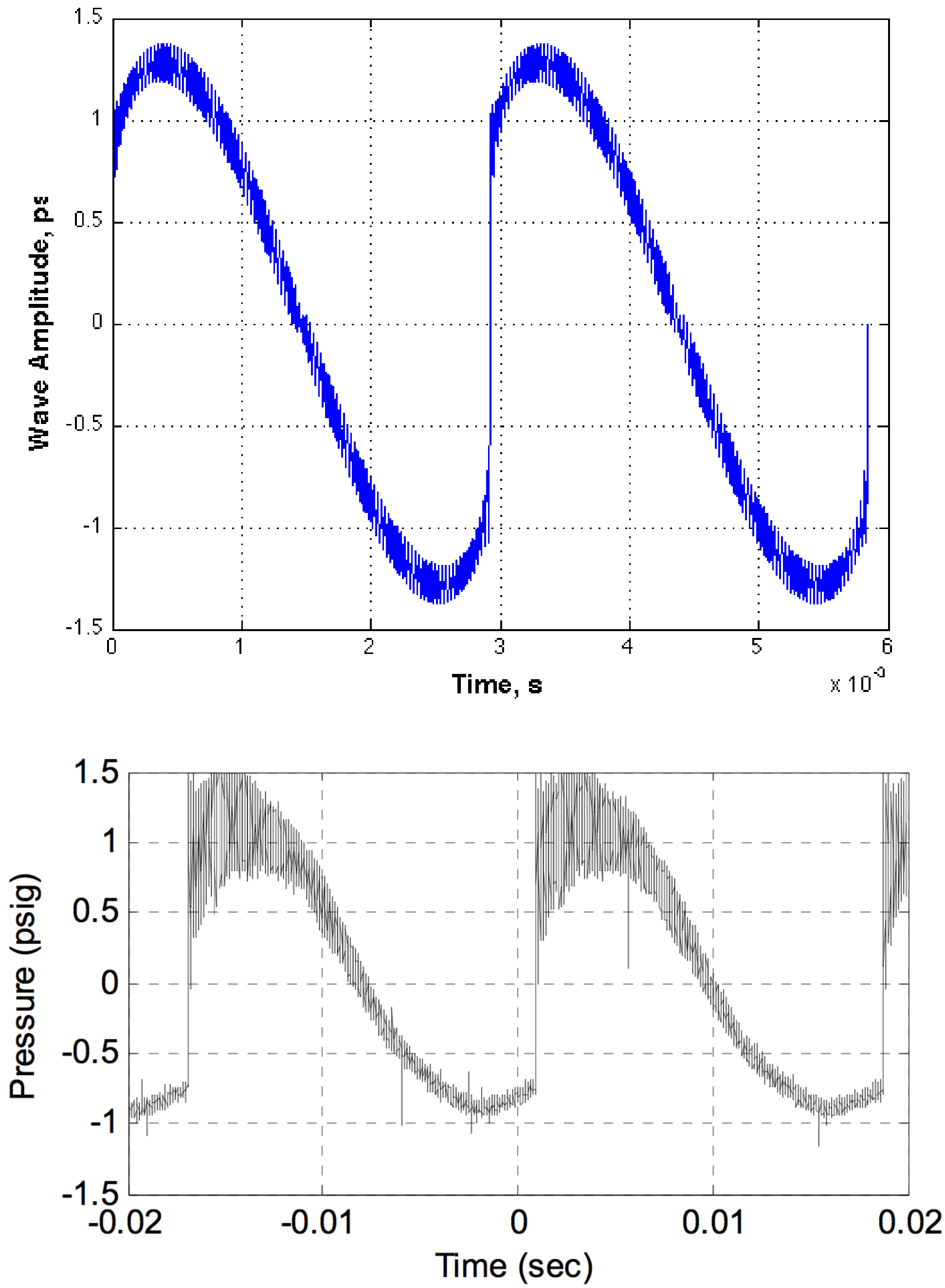


Figure 6.1: Predicted and observed waveforms for Dr. Jacob's experiment

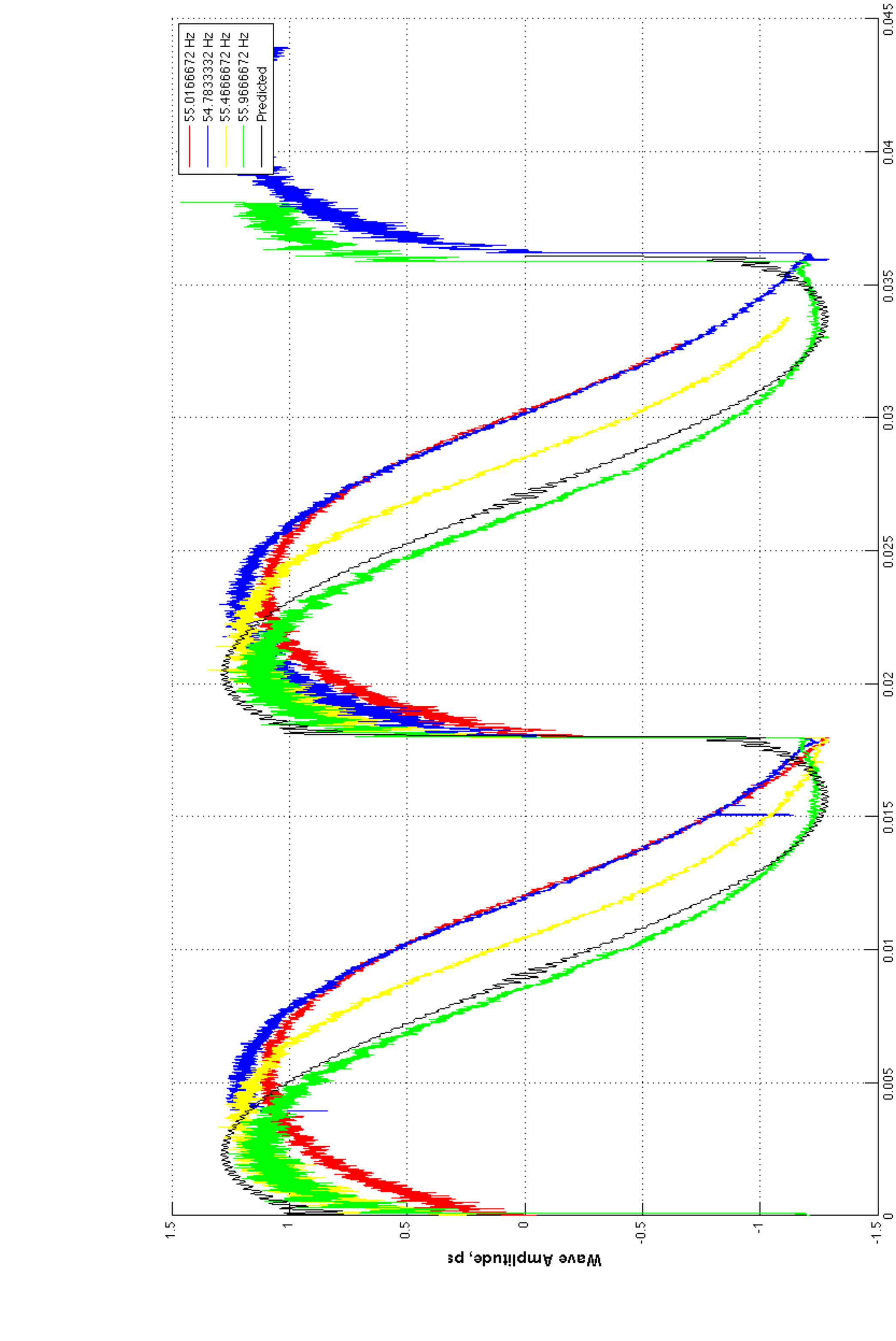


Figure 6.2: Comparison between predicted and observed oscillations in air.

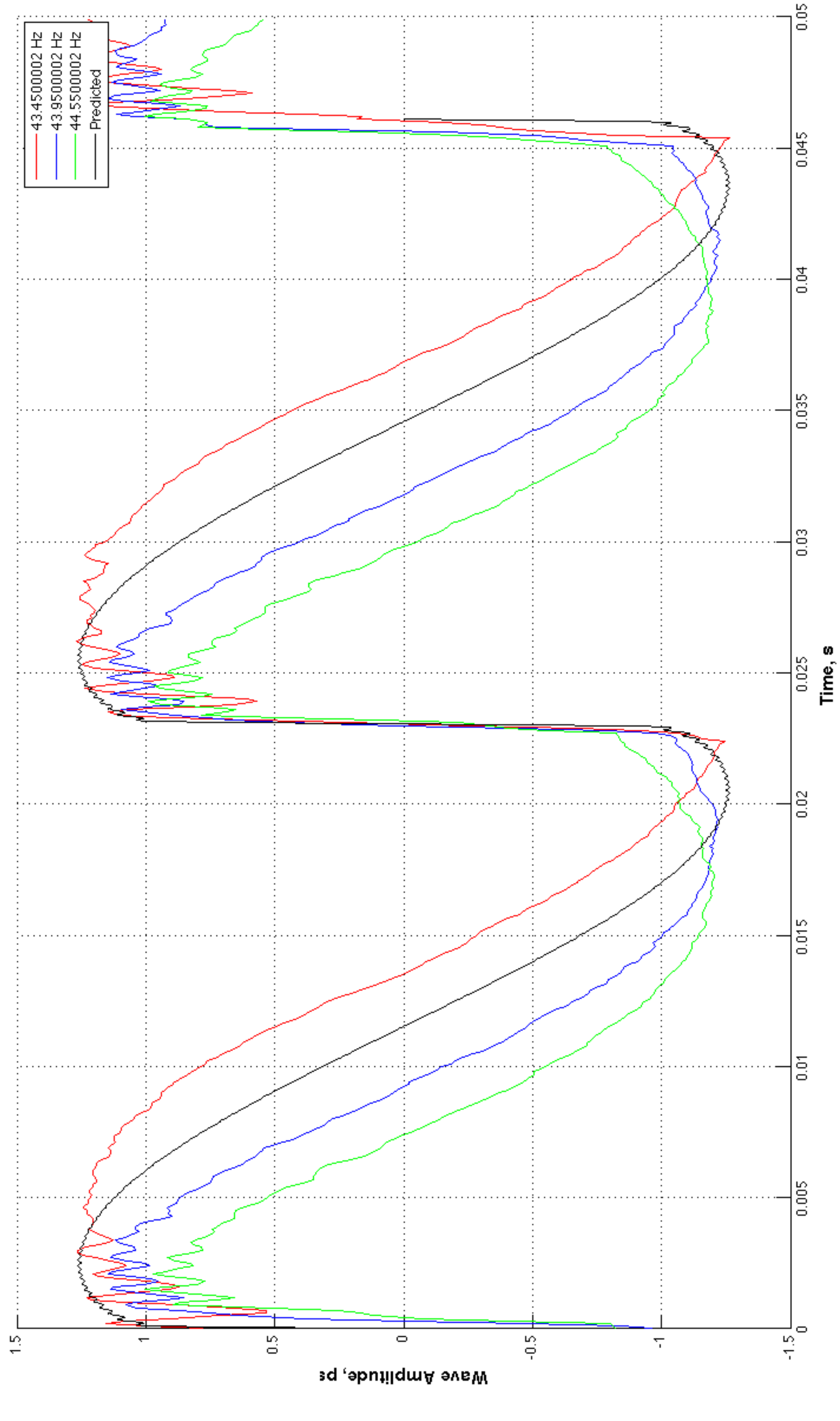


Figure 6.3: Comparison between predicted and observed oscillations in carbon dioxide.

## Bibliography

# Bibliography


[1] G. A. Flandro, "On the oscillatory behavior of liquid propellant rockets," *Advancements in Energetic Materials and Chemical Propulsion*, pp. 320–363, 2008.

[2] E. J. Jacob, *A Study of Nonlinear Combustion Instability.* PhD dissertation, The University of Tennessee Space Institute, 2009.

[3] E. J. Jacob, G. A. Flandro, and D. Banuti, "Forced resonant shock waves and mean pressure shift in a closed tube," *AIAA Paper, 43rd Joint Propulsion Conference*, July 2007.

[4] W. Chester, "Resonant oscillations in closed tubes," *Journal of Fluid Mechanics*, vol. 18, July 1963.

[5] R. Betchov, "Nonlinear oscillations of a column of gas," *The Physics of Fluids*, vol. 1, no. 3, pp. 205–212.

[6] S. Temkin, "Nonlinear gas oscillations in a resonant tube," *The Physics of Fluids*, vol. 11, no. 5, pp. 960–963.

[7] F. Culick, *Unsteady Motions in Combustion Chambers for Propulsion Systems.* RTO/NATO, December 2006.

[8] R. H. Cantrall and R. W. Hart, "Interaction between sound and flow in acoustic cavities: Mass, momentum, and energy considerations," *Journal of the Acoustics Society of America*, vol. 36, no. 4, pp. 697–706.

[9] M. K. Myers, "Transport of energy by disturbances in arbitrary steady flows," *Journal of Fluid Mechanics*, vol. 226, pp. 383–400, 1991.

[10] R. A. Saenger and G. E. Hudson, "Periodic shock waves in resonating gas columns," *The Journal of the Acoustical Society of America*, vol. 32, August 1960.

[11] H. W. Liepmann and A. Roshko, *Elements of Gasdynamics*. Mineola, New York: Dover Publications Inc., 1957.

[12] A. Quarteroni, R. Sacco, and F. Saleri, *Numerical Mathematics*. Heidelberg: Springer Berlin, 2007.

[13] K. U. I. Philip M. Morse, *Theoretical Acoustics*. New York: McGraw-Hill Book Company, 1968.

# Vita

Andrew William Wilson was born in California and raised in Wisconsin. He was declared a Bachelor of the Arts in Physics and Mathematics at the University of Chicago. He subsequently co-founded Humanized Inc., a company dedicated to designing and implementing innovative and humane human-machine interfaces. After leaving Humanized, Andrew continued his studies at the University of Tennessee Space Institute, where he is currently becoming a Master of Science specializing in aerospace engineering. He intends to pursue a doctoral degree in aerospace engineering, hoping one day to participate in the dream.

The dream of building *big* things. That *move. Really fast.*